Experimental study of surface friction coefficient of coarse-grained soil

Xuepeng Wang[1], Shuguo Zhang[1], Jinzhu Zhou[1], Dongming Li[1] and Yongkang Zhu[2,*]

[1]China State Construction Railway Investment & Engineering Group Co., LTD, Beijing, 100000, China
[2]School of Civil Engineering, Central South University, Changsha, Hunan, 410075, China

*Corresponding author's e-mail:224812266@csu.edu.cn

Abstract. Friction coefficients have a significant impact on the vibratory compaction characteristics of coarse-grained soils during road construction. This study conducted vibratory compaction simulations with varying friction coefficients and quantified the roughness of pebble particles and rubble particles using 3D scanning. Then a series of surface friction experiments were conducted. The results indicate that a higher friction coefficient had a less pronounced effect on dry density. Rubble particles generally exhibits higher roughness levels compared to pebble particles. Rubble particles exhibit much more pronounced local surface irregularities. Additionally, the friction coefficient decreased with increasing relative sliding velocity and normal pressure but increased with greater roughness. These findings reveal the relationship between friction coefficients and surface roughness, as well as the relative motion and interaction between particles. They also shed light on how these factors impact the vibratory compaction characteristics of coarse-grained soil.

Keywords: vibration compaction; coarse-grained soil; friction coefficient; roughness.

1   Introduction

The coarse-grained soil is widely used in subgrade construction. Vibratory compaction is a primary method for subgrade compaction[1], and the friction coefficient between particles is a key factor affecting the characteristics of vibratory compaction[2]. Different types of coarse-grained soils have distinct particle surface morphologies, resulting in varying surface friction coefficients[3]. Existing research had indicated that during the process of vibratory compaction, the friction coefficient between particles is not a constant value. It varies with different relative velocities and normal pressure conditions[4-5]. Therefore, it is necessary to study the surface friction characteristics of different types of coarse-grained soil particles under various relative velocities and normal force conditions.

Existing research has primarily focused on studying the impact of normal pressure, relative sliding velocity on frictional characteristics and shear behaviours through

sliding friction experiments. In terms of normal pressure studies, Hong[6] conducted direct shear tests on four different roughness specimens under five different normal pressure conditions and found that higher normal pressures lead to increased surface wear, with the maximum wear area increasing with increasing normal stresses. Babanouri[7] systematically investigated the effects of normal pressure, joint roughness coefficient, and basic friction angle on the shear behaviours of rocks. Cole[8] conducted sliding friction tests between particles, and the results show that the friction coefficient of particles with low surface roughness decreases with the increase of normal force. Regarding the study of relative sliding velocity, Tang[9] performed multiple direct shear tests on three rough joint specimens to investigate the influence of shear velocity on the shear behaviour of artificial rock joints. The study found that with increasing shear velocity, the peak shear strength decreases slightly. Dang[10] conducted shear tests on basalt under different shear velocities, both under constant normal loads and vibrating normal loads. The study revealed that under constant normal loads, the peak shear strength increases with increasing shear velocity. Concerning surface roughness, Kou[11] conducted direct shear tests on three different initial jointed rock specimens and studied the wear process on the joint surfaces during cyclic shear.

In summary, extensive research has been conducted on the frictional characteristics of coarse-grained soil and rocks. The friction coefficient is influenced by various factors, including particle composition, particle shape, surface roughness, sliding velocity, normal pressure, among others. The friction coefficient has a significant impact on the mechanical behaviour of granular soils. Therefore, this study aims to investigate the influence of friction coefficients on the vibratory compaction characteristics of coarse-grained soil under conditions of consistent gradation, particle shape, and vibration parameters using Discrete Element Method (DEM) simulations. A series of surface friction experiments were conducted for two common types of coarse-grained soils (pebble-grained soil and rubble-grained soil). The study explores the surface friction characteristics of coarse-grained soil particles under different relative sliding velocities and normal pressure conditions. Additionally, the surface roughness of both pebbles and rubbles was measured to examine the impact of different surface roughness on the surface friction characteristics of coarse-grained soil. This study will provide insights into the mechanism of vibratory compaction of coarse-grained soils and contribute to understanding the fundamental principles of friction behaviour of granular materials.

2   DEM simulation of different friction coefficients

2.1   Construction of DEM models

In the field of subgrade compaction, the use of DEM allows for the analysis of the macro-mechanical behaviour of the compaction process from a microscopic mechanics perspective[12]. Therefore, in this study, DEM is employed to investigate the impact of different friction coefficients on the effectiveness of vibratory compaction.

Vibratory loading was then initiated with an amplitude of 400kPa and a vibration frequency of 45Hz. The entire model is shown in the Figure 1.
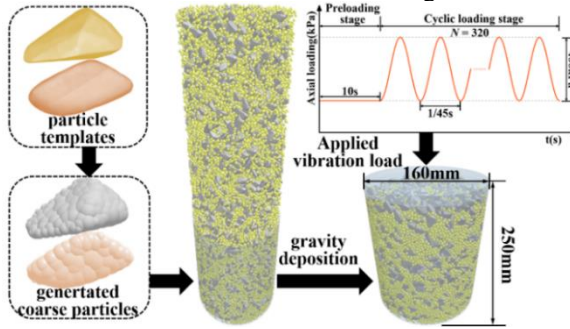

Fig. 1. DEM model generation and vibration load application.

To make the DEM model more representative of actual subgrade compaction projects, the real particle shapes obtained in Section 3.1 were imported into EDEM. The software used an internal particle filling algorithm to populate the particle model's boundaries with sub-spheres, creating clump models that share the same characteristics as the real particle shapes. 8 kg of particles consistent with the gradation in actual engineering were randomly generated. To improve simulation efficiency, particles with diameters less than 5mm were set as spherical particles[13]. Subsequently, these particles were allowed to free-fall into a steel drum with a diameter of 160mm and a height of 250mm. Once stabilized, a rigid loading plate with a diameter of 153mm and a height of 10mm applied a static load of 100kPa to the surface of the sample for 10s. The simulation considered five different sets of friction coefficients between the particles, which were set to 0.1, 0.3, 0.5, 0.7, and 0.9.

2.2   Effect of friction coefficient on vibration compaction characteristics

The evolution of dry density can be used to reflect the vibration compaction characteristics of coarse-grained soil. Figure 2 and Figure 3 depict the variations in dry density over vibration time and the relationship between dry density and friction coefficient, respectively. The dry density exhibits three distinct phases: a rapid increase phase, a gradual increase phase, and a stable phase, as dry density increases rapidly at first, followed by a slower increase until it eventually stabilizes. This pattern aligns with the results of Ye's[14] indoor vibratory compaction experiments. The final dry density decreases as the friction coefficient increases. When the friction coefficient is less than 0.5, it has a more significant impact on dry density. However, when the friction coefficient exceeds 0.5, its influence on dry density significantly diminishes. It is evident that the friction coefficient has a considerable impact on the final dry density. Hence, it is necessary to explore the factors affecting the surface friction coefficient of coarse-grained soil during the vibratory compaction process.
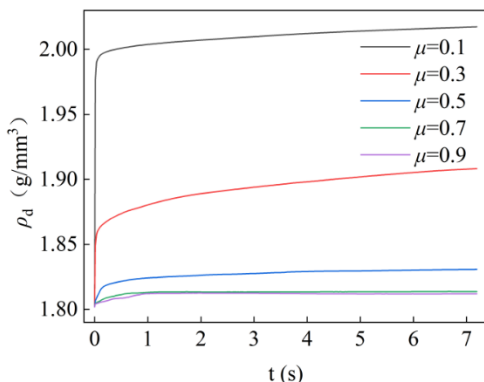
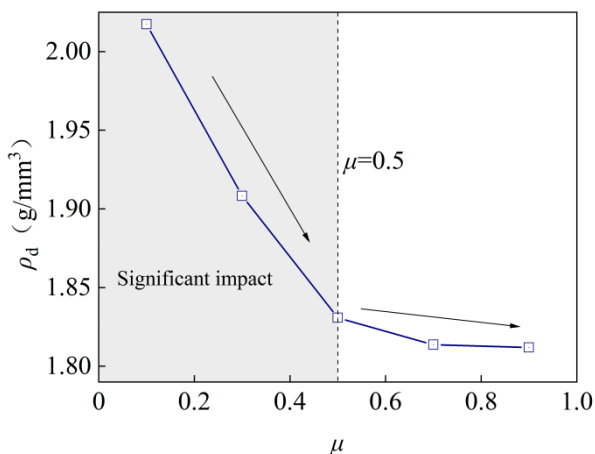**Fig. 2.** Evolution curves of dry density with vibration time.

Fig. 3. Evolution curves of dry density with friction coefficient

3   Test materials, instruments and methods

3.1   Test material and quantification of particle surface roughness

The test materials used in this study were obtained from a road construction site, in-cluding pebble-grained soil and rubble-grained soil. To meet the size requirements of the experimental equipment, 25 kg samples of the pebble-grained soil and rubble-grained soil were separately subjected to sieve analysis. Twenty particles with particle sizes in the range of 10-20 mm were selected from each type. To prevent the influ-ence of dust and fine particles adhering to the surface of particles on the test results, the sieved particles were initially washed with water and then dried in an oven for 24 hours for later use.

To obtain the surface roughness of pebble particles and rubble particles, this study endeavours to quantify the shape indices of particles. Currently, 3D laser scanning

technology has been widely employed to capture the real shape of coarse particles[15-16]. In this study, an automated dual-axis 3D laser scanner was used to scan 200 pebble particles and 200 rubble particles.

The index of roughness is to describe the local fluctuation degree of the particle surface, which is an important factor affecting the interface friction between particles[17]. The calculation formula of roughness is as follows[18]:

$$R_g = \frac{\Delta \bar{d}}{\bar{r}} = \left(\frac{4\pi}{3V_P}\right)^{1/3} \times \frac{1}{S}\sum_{i=1}^{N_d} \Delta d_i \times S_i \tag{1}$$

Where S_i represents the area of the i-th triangular facet, N_d is the total number of triangular facets, d_i denotes the deviation distance of the i-th triangular facet from the reference surface, r represents the average radius of the particles, and V_P is the particle volume.

The probability distribution for calculating the roughness indexes of pebble particles and rubble particles respectively is shown in the Figure 4. The roughness of pebble particles varies approximately between 0 and 0.005, while the roughness of rubble particles varies roughly between 0.005 and 0.015. Rubble particles exhibit much more pronounced local surface irregularities compared to pebble particles. When examining the shape of the probability density distribution curves, the curve for pebble particles is narrower, indicating that pebbles are generally smoother overall. In contrast, the roughness distribution curve for rubble particles is broader and flatter, suggesting greater variability in roughness among rubble particles. Due to the limited range of roughness variation, it is considered that the average roughness values for pebbles and rubbles stone can be taken, with values of 0.002 and 0.009, respectively.
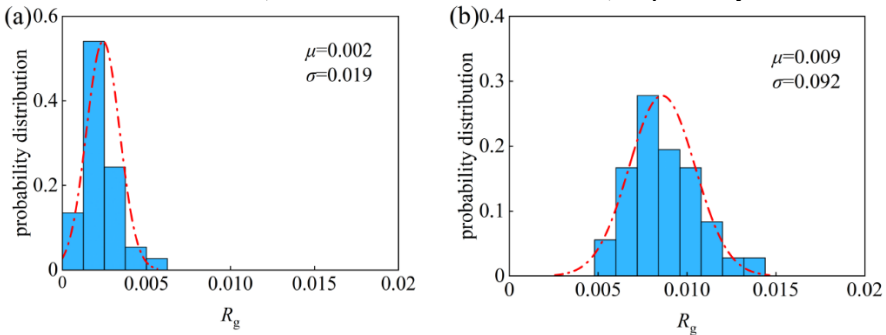

Fig. 4. Probability distributions of R_g for (a) Pebbles and (b) Rubbles.

3.2   Test instruments and methods

The surface friction tests in this study were conducted using a friction and wear testing machine. This instrument primarily consists of modules such as an LVDT (Linear Variable Differential Transformer) displacement sensor, an integrated pressure sensor, a high-precision self-calibrating motor system, a symmetrical elastic cantilever, and a control console (Figure 5). It employs a weight-loading mechanism and a symmetrical cantilever design to ensure load balance and stability. The instrument can

apply a maximum normal load of 10N and has a rotational speed range from 0 to 1200 rpm. Relative sliding between the friction pair and the test specimen generates tangential forces, which can be measured in real-time by monitoring the minute displacements of the symmetrical elastic cantilever, allowing for the real-time measurement of the friction coefficient.
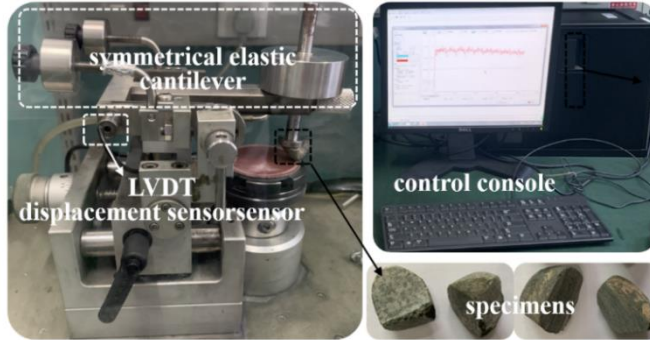
Fig. 5. Schematic diagram of friction and wear testing machine.

According to the requirements of the testing instrument, the dimensions of the friction pair consist of a 60mm diameter and a 4mm height circular disc made of diamond material. Diamond was chosen for its smooth surface, which closely resembles the particle surfaces, and its sufficient hardness, making it suitable for use as the friction pair material. Considering the actual pressures and relative velocities of particles during vibratory compaction, the normal pressure (F_N) and relative sliding velocity (v_r) for the particles were determined based on DEM simulation results. Sixteen sets of tests were conducted, with F_N ranging from 0 to 5N and v_r ranging from 0 to 20mm/s, as shown in Table 1. Each test involved a sliding displacement of 50cm.

**Table 1.** Setting of test conditions for pebbles and rubbles.

| Type of particles	F_N(N)	v_r(mm/s)
Pebble particles	1/3/5	1/5/10/15/20
Rubble particles	3	10

4   Analysis of surface friction characteristics

4.1   Effect of normal pressure on friction coefficient

Figure 6 illustrates the variation of the friction coefficient with sliding displacement at different relative sliding velocities. The friction coefficient first increases to a peak value and then gradually decreases, approaching a plateau. This behaviour is attributed to the uneven distribution of surface asperities on the particles, with only a portion of the area making contact during the sliding process. As sliding displacement increases, the interlocking forces between asperities gradually increase, causing the friction coefficient to rise to its peak. With further sliding displacement, the asperities

in the contact region are sheared, resulting in a decrease in the friction coefficient. As surface asperities wear and accumulate, the particle surface gradually matches the surface of the friction pair, leading to a stabilized friction coefficient. The friction coefficient exhibits continuous fluctuations during the sliding process because each shear of an asperity on the particle's surface is an energy release process. As asperities are continually sheared and worn flat during the sliding friction process, the friction coefficient fluctuates[19]. From Figure 7, it can be observed that both the peak friction coefficient and the average friction coefficient decrease as the relative sliding velocity increases. The reduction in the friction coefficient is more pronounced at lower relative sliding velocities, indicating that it is more significantly affected by changes in relative sliding velocity under such conditions.
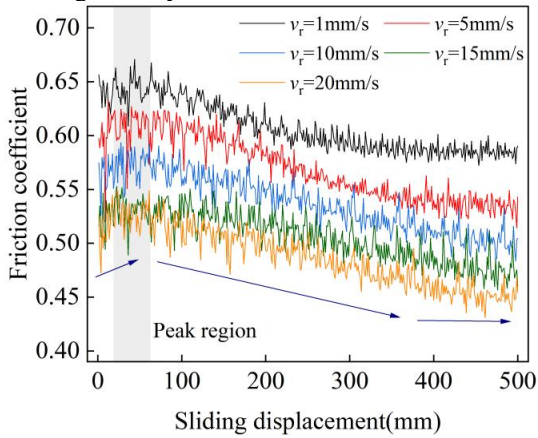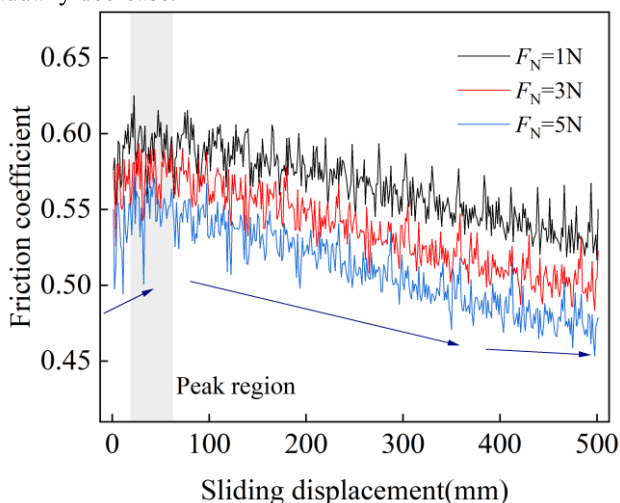

Fig. 6. Evolution of friction coefficient with sliding displacement at different relative sliding velocities.
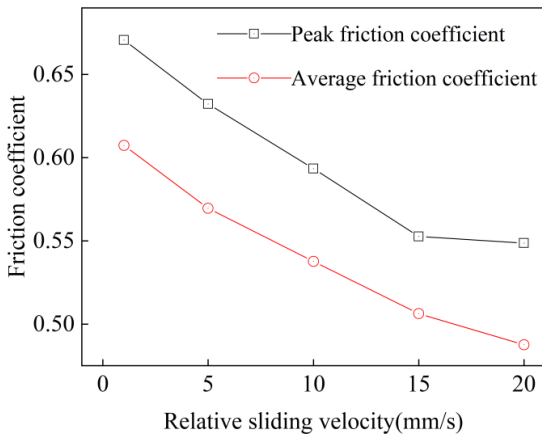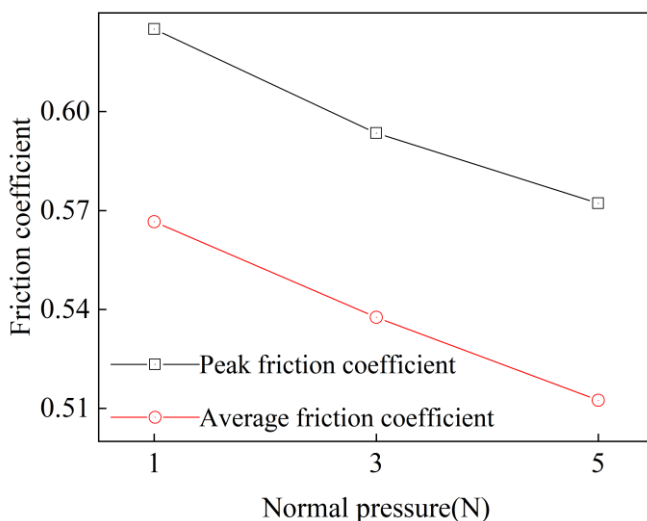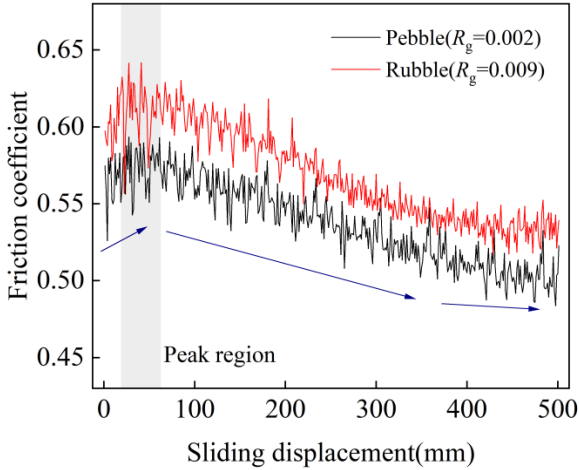

Fig. 7. Evolution of friction coefficient with relative sliding velocity.

4.2   Effect of relative sliding velocity on friction coefficient

Figure 8 presents the evolution of the friction coefficient with sliding displacement at a constant relative sliding velocity of 10mm/s under different normal pressures. Similarly, the friction coefficient first increases to its peak value and then gradually decreases, approaching a plateau. Combining this with Figure 9, it is evident that as the normal pressure increases, both the peak friction coefficient and the average friction coefficient gradually decrease.

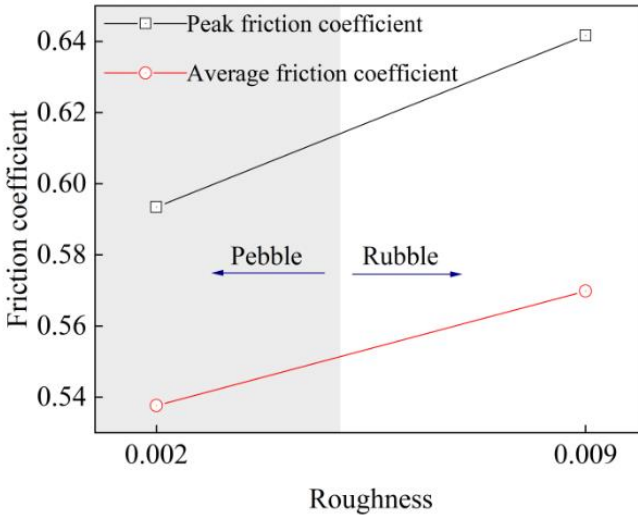**Fig. 8.** Evolution of friction coefficient with sliding displacement at different normal pressure.

Fig. 9. Evolution of friction coefficient with relative normal pressure.

4.3   Effect of surface roughness on friction coefficient

Figure 10 illustrates the evolution of the friction coefficient with sliding displacement for both pebble particle and rubble particle. The friction coefficient first increases to its peak value and then gradually decreases, approaching a plateau. From Figure 11, it can be observed that larger roughness implies a greater number and height of surface asperities on the particles, resulting in a higher friction coefficient. In general, the roughness of rubble particles is greater than that of pebble particles, the friction coefficient of rubble particles is higher than that of rubble particles.

Fig. 10. Evolution of friction coefficient with sliding displacement at different roughness.

Fig. 11. Evolution of friction coefficient with roughness.

5   Conclusion

This study primarily conducted numerical simulations with varying friction coefficients. It quantified the roughness indicators of pebble particles and rubble particles through three-dimensional scanning and subsequently performed a series of surface friction tests. The main conclusions drawn from this study are as follows:

1. The final dry density decreases as the friction coefficient increases. The higher the friction coefficient, the less pronounced its effect on dry density.
2. The roughness of pebble particles varies approximately between 0 and 0.005, while the roughness of rubble particles varies roughly between 0.005 and 0.015. Rubble particles exhibit much more pronounced local surface irregularities compared to pebble particles.
3. The friction coefficient decreases as the relative sliding velocity increases, decreases as the normal pressure increases, and increases as the roughness increases. The roughness of rubble particles is greater than the roughness of pebble particles.

Acknowledgments

References

1. Minaev O. P. (2011) Development of Vibratory Method for Soil Compaction During Construction. Soil Mech. Found. Eng., 48; 190–5.
2. Wei J., Ren J., Fu H. (2022) The weakening of inter-particle friction and its effect on mechanical behaviors of granular soils. Computers and Geotechnics, 147: 104764.
3. Cavarretta I., Coop M., O'sullivan C. (2010) The influence of particle characteristics on the behaviour of coarse-grained soils. Géotechnique, 60: 413–23.
4. Meng F., Liu H., Hua S., Pang M. (2021) Experimental Research on Sliding Friction of Dense Dry Particles Lubricated Between Parallel Plates. Tribol Lett, 69: 33.
5. Sandeep C. S. and Senetakis K. (2018) Grain-scale mechanics of quartz sand under normal and tangential loading. Tribology International, 117: 261–71.
6. Hong E-S., Kwon T-H., Song K-I., Cho G-C. (2016) Observation of the Degradation Characteristics and Scale of Unevenness on Three-dimensional Artificial Rock Joint Surfaces Subjected to Shear. Rock Mech Rock Eng, 49: 3–17.
7. Babanouri N., Asadizadeh M., Hasan-Alizade Z. (2020) Modelling shear behavior of rock joints: A focus on interaction of influencing parameters. International Journal of Rock Mechanics and Mining Sciences, 134: 104449.
8. Cole D. M. (2015) Laboratory observations of frictional sliding of individual contacts in geologic materials. Granular Matter, 17: 95–110.

9. Tang Z. C. and Wong L. N. Y. (2016) Influences of Normal Loading Rate and Shear Velocity on the Shear Behavior of Artificial Rock Joints. Rock Mech Rock Eng, 49: 2165–72.
10. Dang W., Chen J. and Huang L. (2021) Experimental study on the velocity-dependent frictional resistance of a rough rock fracture exposed to normal load vibrations. Acta Geotech., 16: 2189–202.
11. Kou M., Liu X., Tang S., Wang Y. (2019) Experimental study of the prepeak cyclic shear mechanical behaviors of artificial rock joints with multiscale asperities. Soil Dynamics and Earthquake Engineering, 120: 58–74.
12. Wang Y., Mora P., Liang Y. (2022) Calibration of discrete element modelling: Scaling laws and dimensionless analysis. Particuology, 62: 55–62.
13. Lai R., Xu F., Qi Q., Nie Z. (2023) Exploring the effects of gravel shapes on vibration compaction behaviours of coarse-grained mixtures via DEM simulations. International Journal of Pavement Engineering, 24z: 2201501.
14. Ye, Y., Chen, X., Hui, X., Cai, D., Yao, J., Jin, L. (2021). Laboratory investigation on parameter optimization of vibrating compaction for high-speed railway's Group B. Journal of Railway Science and Engineering, 18: 2497–2505. (in Chinese).
15. Ge H., Quezada J. C., Houerou V. L., Chazallon C. (2021) Three-dimensional simulation of asphalt mixture incorporating aggregate size and morphology distribution based on contact dynamics method. Construction and Building Materials, 302: 124124.
16. Liu D., Sun L., Ma H., Cui W. (2020) Process Simulation and Mesoscopic Analysis of Rockfill Dam Compaction Using Discrete Element Method. Int. J. Geomech., 20: 04020047.
17. Sandeep C. S. and Senetakis K. (2018) Effect of Young's Modulus and Surface Roughness on the Inter-Particle Friction of Granular Materials. Materials, 11: 217.
18. Wang X. (2020) Shape quantification, model reconstruction of geotechnical granular materials and application to discrete element modeling. PhD. (Central South University).
19. Zhao G., Wang L., Zhao N., Yang J., Li X. (2020) Analysis of the Variation of Friction Coefficient of Sandstone Joint in Sliding. Advances in Civil Engineering, 2020: e8863960.